Proc. Budapest'02 Workshop on
Quark & Hadron Dynamics (2002) 000–000

Budapest'02 Workshop on
Quark & Hadron Dynamics
Budapest, Hungary
March 3–7, 2002

QGP Hydrodynamics for RHIC Energies

L.P. Csernai,[1,2] C. Anderlik,[3] A. Keranen,[4]
V.K. Magas,[5] J. Manninen[4] and D.D. Strottman[6]

[1] Theoretical and Computational Physics Section, University of Bergen
Allegaten 55, N-5007 Bergen, Norway
[2] KFKI Research Institute for Particle and Nuclear Physics
P.O.Box 49, H-1525 Budapest 114, Hungary
[3] Parallab, Computational Science & High Performance Computing Laboratory
University of Bergen, N-5020 Bergen, Norway
[4] Department of Physical Sciences, P.O.Box 3000, FIN-90014
University of Oulu, Finland
[5] Center for Physics of Fundamental Interaction, Physics Department
Instituto Superior Tecnico, Av. Rovisco Pais, 1049-001 Lisbon, Portugal
[6] Theory Division, Los Alamos National Laboratory,
Los Alamos, NM 87545, USA

Abstract. The relativistic hydrodynamic approach in this field became one of the best established theoretical and experimental methods.[1] The applicability of this method is vital, so we have to discuss the initial and final stages of heavy ion reactions in great detail, in addition to the middle stages of the reaction where the relativistic hydrodynamic description provides an adequate and accurate description of the reaction.

Keywords: Relativistic Hydrodynamics, Heavy Ion Reactions
PACS: 25.75.-q, 25.75.Ld, 24.10.Nz

1. Introduction

At SPS and RHIC more "stopping" is observed than was anticipated earlier, [2, 3] and the abundances of strange hadrons, particularly of anti-strange baryons, are enhanced. These observations led to modeling changes, new "energetic" degrees of freedom: string ropes, fused strings, quark clusters, were introduced in Monte-Carlo sting models to cope with these observations. These indicate the occurrence of quark-gluon plasma effects or can be considered as its precursors.

Any model that we want to apply must fit what is already confirmed. First of all, it is well known by now, that ultra-relativistic nuclear collisions show strong stopping, and this supports and justifies the use of one-fluid, fluid dynamical models, which assume a complete stopping. Of course Fluid Dynamics (FD) should be used only after stopping or local equilibration is achieved. At ultra-relativistic energies this does not happen instantly.

We should pay attention to basic principles of physics when modeling complicated processes as heavy ion collisions.

2. Multi Module Model

A realistic and detailed description of an energetic heavy ion reaction requires a Multi Module Model, where the different stages of the reaction are each described with a suitable theoretical approach.[4] It is important that these modules are coupled to each other correctly: on the interface, all conservation laws should be satisfied, and the entropy should not decrease. This last feature sometimes not given proper attention. The increasing entropy condition should be satisfied at each "stage" or "Module" of our collision model, as well as, at the transition between stages or modules.

The initial and final, Freeze-Out (FO), stages of reaction are outside the domain of the applicability of the fluid dynamical model. After hadronization and FO, the matter is already dilute and can be described well with kinetic models. The initial stages are the most problematic. None of the theoretical models can unambiguously describe the initial stages. Since we cannot describe unambiguously the initial stages, we have to use some phenomenological models. There are two phenomenological models that are frequently used: the Landau model (which describes complete stopping) and the Bjorken model (which describes complete transparency). Here we describe the initial state with the Effective String Rope Model (ESRM).[4, 5] Both these models utilize an earlier model of the string dynamics described in ref. [6]. Then, the hydrodynamic evolution with a QGP EoS is used for the intermediate state.

The initial dynamics using the effective string rope model led to an initial state with high energy density, reaching 20 GeV/fm^3 on the average and 60-80 Gev/fm^3 peak values in the middle. This coincides with other estimates based on the first flow results at RHIC. Due to the assumption of uniform energy and baryon charge distribution within each string the surface of the initial configuration did cut off to zero sharply at the surface. In the first 3 dimensional Computational Fluid Dynamical (CFD) calculations this (not very physical) assumption led to a huge pressure gradient at the surface, which created two sharp forward/backward moving, leading peaks, just as if we would have had a highly transparent collision. Otherwise, the initial state model led to a configuration which was similar to the initial state described in Landau's fluid dynamical model, with the difference that the relatively flat initial state was tilted. In a heavy ion reaction such a tilted initial state arises naturally as a consequence of the streak by streak momentum conservation, since at finite impact parameters streaks with different length and mass collide against each other, finally moving in the direction of the heavier streak.

Such a tilted flat initial state results in a "third flow component" which is observed at the highest SPS energies, and it was present in all FD model results which used QGP EoS. We have also improved the initial state by also considering some expansion during the formation of the initial state, to avoid the artifacts arising from the irrealisticly sharp surface pressure drop. The resulting smoother initial energy distribution is shown in Figure 1

2.1. Numerical 3-Dimensional CFD results for RHIC Energies

With the improved initial condition, the PIC-method used by the Bergen - Los Alamos collaboration was also upgraded to increase stability. As due to the extreme Lorentz contraction increasing the cell size was out of question, stability was increased by introducing randomly positioned "marker particles" (Lagrangian Fluid Cells) in the model. This reduced the sensitivity to grid related instabilities to a large extent. We also used a Bag Model EoS, which enabled supercooling, in contract to the earlier tabulated EoS created by Maxwell Construction which assumed necessarily phase equilibrium. We had no hadronic matter EoS in the model at all, surface effects were neglected, and the Quark matter necessarily supercooled during the final expansion in the FD stage of the reaction.

Starting out from the initial state obtained from the Effective String Rope Model, we arrived at a typical flow pattern, the "third flow component".

2.2. The Third Flow Component

The third flow component does arise from a flat compressed and TILTED initial state. The flat initial state then expands in the reaction plane orthogonal to the directed flow. This effect is also a QGP signal, because to form a rather flat initial state we need a highly compressible matter like QGP with reduced pressure. When the Third Flow Component was first identified [7], it was also observed that ALL FD model calculations have predicted this effect with QGP EoS, independent of each other. At the same time the same models led to negative results with hadronic matter EoS!

The obtained peaks were rather sharp in the fluid dynamical model calculation because we did not take into account the random thermal motion of particles. This we can do in the final Freeze Out (FO) module of our reaction model.

2.3. The Cooper-Frye Freeze Out Model

The first attempt to solve the FO problem, and to calculate the observables was made by Landau [10]. He just evaluated the flow velocity distribution at freeze-out, and this distribution served as a basis of all observables. This approach was used in

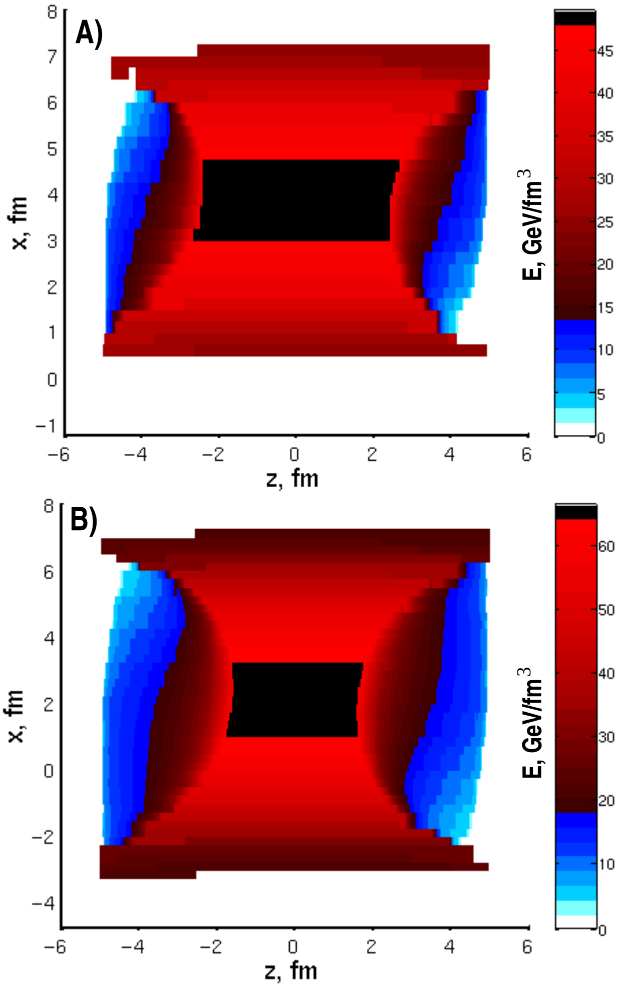

Fig. 1. Au+Au collision at $\varepsilon_0 = 100\ GeV/nucl$, $E = T^{00}$ is presented in the reaction plane as a function of x and z for $t_h = 5\ fm/c$. Subplot A) ($b = 0.5 \cdot 2\ R_{Au}$), subplot B) ($b = 0.25 \cdot 2\ R_{Au}$). The QGP volume has a shape of a tilted disk and may produce a third flow component. From [5].

early FD simulations of heavy ion collisions, but it was not a very good one because in this model the system loses energy due to the neglected local random thermal motion, so energy conservation is violated. Milekhin [11,12] included thermal energy in evaluation of mesurables, adding random thermal velocities to the flow at FO. Although this procedure was still not exact. The FO model was improved later by Cooper and Frye [13] and this method is widely used ever since.

However, the method obtained by Cooper and Frye still did not provide a complete solution to the problem, and some typical mistakes appear in almost all FO calculations [14].

As we know, the FO across a hypersurface is a discontinuity and, the energy-momentum tensor changes discontinuously across this surface. If the flow is not orthogonal to this surface, the four-velocity of the flow will also change [16]. The invariant number of particles (world lines) crossing a surface element $d\sigma^\mu$ is

$$dN = N^\mu d\sigma^\mu \tag{1}$$

and the total number of all particles crossing this surface is

$$N = \int_S N^\mu \; d\sigma_\mu \; . \tag{2}$$

This total number, N, and the total energy and momentum are of course the same at both sides of the freeze out surface.

If we insert the kinetic definition of N^μ

$$N^\mu = \int \frac{d^3p}{p^0} \; p^\mu \; f_{FO}(x,p;T,n,u^\nu) \; ,$$

into eq.(1) we obtain the Cooper-Frye formula:

$$E\frac{dN}{d^3p} = \int f_{FO}(x,p;T,n,u^\nu) \; p^\mu d\sigma_\mu \; , \tag{3}$$

where $f_{FO}(x,p;T,n,u^\nu)$ is the post FO phase space distribution of the frozen-out particles, which is not known from FD models. The problem is to choose its form correctly. At this point the original Cooper-Frye model has to be corrected.

2.4. Matching Conditions

To evaluate measurables we have to use the parameters of the matter after the discontinuity. If we know the pre freeze out baryon current and energy-momentum tensor, N_0^μ and $T_0^{\mu\nu}$, we can calculate locally, across a surface element of normal vector $d\sigma^\mu$ the post freeze out quantities, N^μ and $T^{\mu\nu}$, from the matching conditions above [15, 17]:

$$[N^\mu \; d\sigma_\mu] = 0 \; , \quad [T^{\mu\nu} \; d\sigma_\mu] = 0 \quad \text{and} \quad [S^\mu \; d\sigma_\mu] \geq 0. \tag{4}$$

Here $[A] \equiv A - A_0$. The first two equations are the conservation laws for N^μ and $T^{\mu\nu}$. The third one tells us that entropy must always increase (here S^μ is the entropy 4-curent). Thus, the post FO distribution has to be chosen so, that these conditions are satisfied. In the Cooper-Fry description it was suggested instead that one should use an ideal gas distribution with the pre FO parameters, u^μ, n and T, which is wrong, and strictly speaking leads to a violation of conservation laws.

2.5. Post Freeze Out Distribution from Matching Conditions

Is usual assume that the pre FO momentum distribution is a local thermal one; boosted by the local collective flow velocity. Nevertheless, the post freeze out distribution need not be a thermal equilibrium distribution.

For time-like freeze out surfaces, we may still assume a thermal distribution (Jüttner or the equivalent for relativistic quantum ideal gases), and this does not lead to any problem, because both p^μ and $d\sigma^\mu$ are time-like unit vectors, so $p^\mu d\sigma_\mu > 0$, (i.e. all frozen out particles will propagate over the FO surface to the post FO side). As a consequence the integrand in eq.(3) is positive on both sides of the front, permitting its application.

Of course, the parameters T, n, u^μ, of the f_{FO} distribution, must be determined from the first two eq. of (4). The third eq. from (4) have to be used just to guarantee reliable solutions [17]. These important conditions were missed in the original work [13] and in many applications since.

In case of a space-like FO surface the situation is more complicated. Here p^μ is time-like and $d\sigma^\mu$ is space-like, thus $p^\mu d\sigma_\mu$ can be both positive or negative, and $d\sigma^\mu$ may point now both in post- and pre- FO directions. Thus, the integrand in eq.(3) may change sign, indicating that the distribution has contributions back into-, and also out of the front.

On the pre FO side particles may move in any direction and may rescatter on each other. However, on the post freeze out side, we do not allow re- and back-scattering any more. In other words a particle cannot scatter back if it has passed the FO front. So, the post-FO distribution should have the form [17]:

$$f^*_{FO}(x,p;T,n,u^\nu,d\sigma^\mu) = f_{FO}(x,p;T,n,u^\nu)\Theta(p^\mu\ d\sigma_\mu) \qquad (5)$$

where $\Theta(p^\mu\ d\sigma_\mu)$is the step function. Thus, f^*_{FO} *cannot be a Jüttner or other ideal gas distribution.* Nevertheless, conservation laws have to be satisfied, even in this case. This problem was addressed and solved in a series of publications. [19–23]

2.6. Sudden Hadronization in Freeze Out

Although, the freeze-out, is primarily not an equilibrium process, we can use a Canonical or Grand Canonical statistical model to estimate hadron abundances post FO. This is based on the assumption that the statistical ensemble we use is close to the ensemble formed in a series of experiments, where the global experimental parameters (e.g. energy, impact parameter) were the same, and the nonstatistical factors in the formation probability of the hadrons are similar. (This latter condition is not applicable to some, but only very few, hadrons.) Such a model can then be used at the end of an FD calculation for each fluid cell separately.

Fof purposes of demonstration this was done in ref. [24], in a simple Bjorken type expansion model, where the Freeze Out happened at a constant time. The matter was originally in QGP phase, and then suddenly Froze Our and Hadronized. The resulting hadron gas had different parametes at different positions along the beam (z) axis. Of course the flow velocity has changed, and all thermodynamical parameters of the matter.

Three different pre FO equations of State were assumed (see [24] (a), (b), and (c)), and in case (a) the entropy decreased, in case (b) the hadronic matter was superheated everywhere, only in case (c) could one satisfy all conditions of FO, but for $z < 6$fm only. See Figure 2.

2.7. Determining the reaction plane at RHIC

Finally let us discuss an experimental problem which was discussed during this workshop.

At RHIC the directed transverse flow was not measured up to now. Different experimental difficulties were mentioned as the reason. In particular that the reaction plane could not be identified, although the so called v_2 parameter was measured.

This problem is partly due to the method used to determine v_2, which did not explicitly required the parallel determination of the reaction plane. It is, however, clear that the existence of strong elliptic flow indicates a strong collective correlation among the particles in every event: particles are preferably emitted upwards (+x) and downwards (-x) in the reaction plane and much less to the sides. Thus, if this correlation is detected and strong, the plane must be identifiable also! It is relatively easy to design methods, which work well statistically for very low event multiplicities.

Of course, to tell which is the target and projectile side of the plane may be difficult. If in a symmetric, A+A reaction one assumes, the idealized Bjorken picture with infinite length in the [z]-direction, and the lens shape source in the transverse plane, the target and projectile side cannot be distinguished in principle.

On the other hand, if one takes a more realistic three dimensional model, one will get both azimuthal asymmetry and forward/backward asymmetry. This can be used then to determine which side of the plane is which.

As v_2 is measured, the reaction plane, [x,z], is known, just the target/projectile side should be selected. This is not done due to the prejudice that the distribution of emitted particles is mirror-symmetric in CM:

$$f_{CM}(p_x, p_y, p_z) = f_{CM}(p_x, p_y, -p_z)$$

However, at finite impact parameters (2-15%) there is a fwd / bwd asymmetry, which utilize the following way to determine the reaction plane.

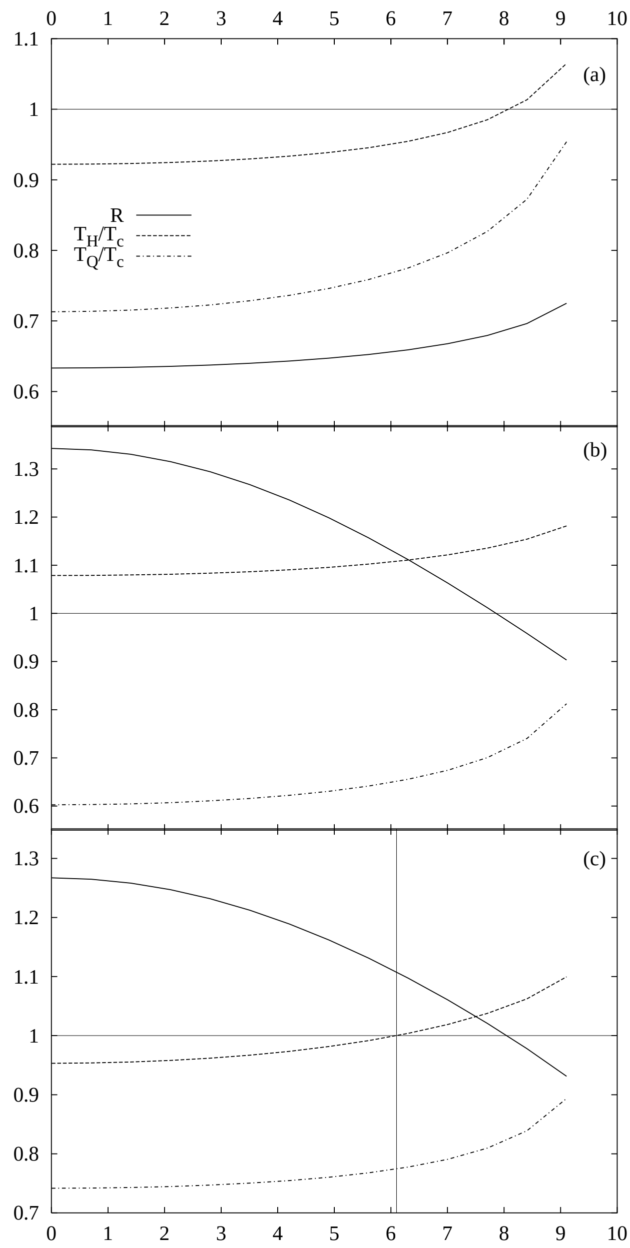

Fig. 2. Various quantities on the FO surface. Panels from top to bottom: a) ideal gas EoS for QGP, b) MIT bag EoS, c) spinodal EoS. R is the ratio of entropy currents in HG and QGP, T_H and T_Q are the temperatures on the HG and QGP side, and T_c is the critical temperature. The model parameters in the bag- and spinodal EoS are fixed to produce critical temperature 160 MeV. For the ideal gas EoS, there is no real T_c, the chosen 160 MeV is arbitrary. The vertical line in the panel c marks the point, where the HG temperature crosses the critical value. From [24].

Let us calculate, event by event, the Q-vector (a la Danielewicz, and Odyniecz (1985), see in section 7.7 of ref. [1]):

$$Q_k = \sum_{ik} y_{CM,i} p_{x,i}$$

for all particles, i, of type k. Only the sign is relevant, as the plane is known already. This Q-vector will select the same side (e.g. projectile) in each event.

3. Conclusions

In conclusion we can state that hydrodynamic modeling of heavy ion reactions is alive and is better than ever. Clear hydrodynamic effects are seen everywhere, and from early on.

This indicates we are approaching a regime where collective matter type of behavior is dominant. We hope to gain more and more detailed information on QGP and its dynamical properties. Continued hard work is needed to exploit all possibilities, and the task of theoretical modeling and analysis is vital in future progress of the field.

Acknowledgements

Three of us (A.K., V.M. and D.S.) acknowledge the support of the Bergen Computational Physics Laboratory in the framework of the European Community - Access to Research Infrastructure action of the Improving Human Potential Programme.

References

1. L.P. Csernai: *Introduction to Rel. Heavy Ion Collisions*, Willey (1994).
2. L.P. Csernai, J.I. Kapusta, *Phys. Rev.* **D29** 2664. (1984).
3. L.P. Csernai, J.I. Kapusta, *Phys. Rev.* **D31** 2795. (1985).
4. V.K. Magas, L.P. Csernai, D.D. Strottman, *Phys. Rev.* **C64** 014901, (hep-ph/0010307) (2001).
5. V.K. Magas, L.P. Csernai, D. Strottman, Submitted to *Physical Review* **C** , (hep-ph/0202085) (2002).
6. M. Gyulassy, L.P. Csernai: *Nucl. Phys.* **A 460** 723 (1986).
7. L.P. Csernai and D. Röhrich, *Phys. Lett.* **B458** 454. (nucl-th/9908034) (1999).
8. L.P. Csernai and J.I. Kapusta, *Phys. Rev.* **D46** 1379 (1992); and L.P. Csernai and J.I. Kapusta, *Phys. Rev. Lett.* **69** 737. (1992).
9. L.P. Csernai and I.N. Mishustin, *Phys. Rev. Lett.* **74** 5005. (1995).
10. L.D. Landau, Izv. Akad. Nauk SSSR **17** (1953).
11. G. Milekhin, Zh. Eksp. Teor. Fiz. **35** 1185 (1958); Sov. Phys.-JETP **35** 829 (1959).
12. G. Milekhin, Trudy FIAN **16** 51 (1961).

13. F. Cooper and G. Frye, Phys. Rev. **D 10** 186. (1974).
14. L.P. Csernai, Zs. Lázár and D. Molnár, *Heavy Ion Phys.* **5** 467. (1997).
15. L.P. Csernai, Sov. JETP **65** 216 (1987); Zh. Eksp. Theor. Fiz. **92** 379. (1987).
16. T. Csörgő and L.P. Csernai, *Phys. Lett.* **B333** 494. (hep-ph/9406365), (1994).
17. Cs.Anderlik, L.P.Csernai, F.Grassi, W.Greiner, Y.Hama, T.Kodama, Zs.Lázár,V. Magas and H. Stöcker, *Phys. Rev.* **C59** 3309. (nucl-th/9806004) (1999).
18. A.H. Taub, Phys. Rev. **74** 328. (1948).
19. K.A. Bugaev, *Nucl. Phys.* **A606** 559. (1996).
20. Cs. Anderlik, Z.I. Lázár, V.K. Magas, L.P. Csernai, H. Stöcker and W. Greiner, *Phys. Rev.*, **C59** 388, (nucl-th/9808024) (1999).
21. V.K. Magas, Cs. Anderlik, L.P. Csernai, F. Grassi, W. Greiner, Y. Hama, T. Kodama, Zs. Lázár and H. Stöcker, *Nucl. Phys.* **A661** 596. (nucl-th/0001049) (1999).
22. V.K. Magas, et al. *Phys. Lett.* B **459** 33, (nucl-th/9905054); (1999).
23. V.K. Magas, Cs. Anderlik, L.P. Csernai, F. Grassi, W. Greiner, Y. Hama, T. Kodama, Zs. Lázár and H. Stöcker, *Heavy Ion Phys.* **9** 193. (nucl-th/9903045) (1999).
24. A. Keranen, L.P. Csernai, V. Magas and J. Manninen, Submitted to *Physical Review* **C** (2002) , (nucl-th/0205019).